Article:
Fan, XZ, Wang, YY, Cui, ZY et al. (2022) Kv7.4 channel is a key regulator of vascular inflammation and remodeling in neointimal hyperplasia and abdominal aortic aneurysms. Free Radical Biology and Medicine, 178. pp. 111-124. ISSN: 0891-5849

https://doi.org/10.1016/j.freeradbiomed.2021.11.041

Kv7.4 channel is a key regulator of vascular inflammation and remodeling in neointimal hyperplasia and abdominal aortic aneurysms

Xi-zhenzi Fan[a#], Ying-Ying Wang[a#], Zi-Yang Cui[a], Zi-Hao Cheng[a], Hai-Lin Zhang[b], Nikita Gamper[b,c], Fan Zhang[a**], Mei Han[a*]

[a] Department of Biochemistry and Molecular Biology, College of Basic Medicine, Key Laboratory of Medical Biotechnology of Hebei Province, Key Laboratory of Neural and Vascular Biology of Ministry of Education, Hebei Medical University, Shijiazhuang 050017, PR China

[b] Department of Pharmacology, Key Laboratory of Neural and Vascular Biology, Ministry of Education, China; Key Laboratory of New Drug Pharmacology and Toxicology, Hebei Medical University, Shijiazhuang 050017, PR China

[c] School of Biomedical Sciences, Faculty of Biological Sciences, University of Leeds, Leeds, UK

# These authors contributed equally to this work.

*** Corresponding author.**

****Corresponding author.**

E-mail addresses: hanmei@hebmu.edu.cn (M. Han), zhangfan86@hebmu.edu.cn (F. Zhang)

Abstract

Inflammation has recently emerged as an important contributor for cardiovascular disease development and participates pivotally in the development of neointimal hyperplasia and abdominal aortic aneurysms (AAA) formation. Kv7.4/KCNQ4, a K^+ channel, is one of the important regulators of vascular function but its role in vascular inflammation is unexplored. Here, we showed that the

expression of Kv7.4 channel was elevated in the neointima and AAA tissues from mice and humans. Genetic deletion or pharmacological inhibition of Kv7.4 channel in mice alleviated neointimal hyperplasia and AAA formation via downregulation of a set of vascular inflammation-related genes, matrix metalloproteinases (MMP) 2/9, and intercellular adhesion molecule (ICAM-1). Furthermore, genetic deletion or inhibition of Kv7.4 channel suppressed the activation of tumor necrosis factor receptor 1 (TNFR1)-nuclear factor (NF)-κB signaling pathway via blockade of interaction between TNFR1 and TNFR1-associated death domain protein (TRADD) in vascular smooth muscle cells (VSMCs). Knockdown of Kv7.4 *in vivo* identified VSMCs-expressed Kv7.4 as a major factor in vascular inflammation. Collectively, our findings suggest that Kv7.4 channel aggravates vascular inflammatory response, which promotes the neointimal hyperplasia and AAA formation. Inhibition of Kv7.4 channel may be a novel therapeutic strategy for vascular inflammatory diseases.

Keywords

Kv7.4 channels, Vascular smooth muscle cells, Vascular inflammation, TNFR1 signaling, Neointimal hyperplasia

1. Introduction

Vascular inflammation is an important etiological factor of cardiovascular diseases, such as neointimal hyperplasia and abdominal aortic aneurysms (AAA) [1,2]. Neointimal hyperplasia is a reparative process characterized by the expansion of cellular population within the innermost layer of an artery or vein, whereby different inflammatory factors and cells stimulate proliferation and migration of vascular smooth muscle cells (VSMCs) from the tunica media [3,4]. AAA is a permanent and localized dilatation of the abdominal aorta that exceeds the normal diameter by >50%. The AAA pathology is characterized by the increased inflammatory cell infiltration, aberrant oxidative stress, medial elastin degradation and medial collagen deposition [5]. Emerging evidences indicate that both neointimal hyperplasia and AAA share common inflammatory triggers, which determine and regulate the onset, progression and outcomes of both these pathologies [2]. Therefore, targeting this inflammatory response could be a promising therapeutic strategy to reduce vascular lesion and reduce neointimal hyperplasia and AAA.

The transcription factor nuclear factor (NF)-κB is an inflammatory marker associated with various inflammatory cardiovascular diseases [6,7]. The initial step leading to activation of NF-κB signaling are triggered by pro-inflammatory cytokine tumor necrosis factor (TNF)-α, which initiates the formation of a complex between the tumor necrosis factor receptor 1 (TNFR1) and the immediate downstream adapter molecule, TNFR1-associated death domain protein (TRADD) [8]. This complex is essential for the subsequent activation of IκB kinases (IKK) complex [9,10]. IκBα phosphorylated by IKK is degraded via ubiquitin-proteasome pathway, thus permitting nuclear translocation of the NF-κB, which activates the expression of pro-inflammatory genes, such as matrix metalloproteinases (MMP2/MMP9) and intercellular adhesion molecule (ICAM-1).

Recent studies have shown an association between ion channel activity and cardiovascular diseases [11]. One of the ion channel types found in the vasculature is the Kv7 channels encoded by *Kcnq* genes. Kv7s (also called M-type) is a subfamily of

voltage-gated potassium channels with a very negative activation threshold (negative to -60 mV), slow kinetics and no inactivation, properties that enables these channels to exert strong control over cell's resting membrane potential and excitability [12,13]. Several Kv7 channels, including Kv7.1, Kv7.4 and Kv7.5, have been identified in various rodent and human blood vessels as key regulators of vascular tone [14,15]. Kv7.1 was the most abundant subunit in a mouse portal vein [16], However, the subsequent studies identified Kv7.4 and Kv7.5 as the major determinants of vascular tone in various types of blood vessels [17-19]. Blockade of Kv7/M channels by their selective inhibitors, XE991 or linopirdine, produced spontaneous contractility in the most arteries and enhanced vasoconstrictor responses [20]. Furthermore, reduction in Kv7.4 channel activity and expression in arterial beds has also been shown to result in hypertension [15]. Thus, Kv7/M channels and Kv7.4 specifically, have been identified as a promising target for treatment of various vascular disorders [21,22]. Yet, the involvement of Kv7/M channels in vascular inflammation is hitherto underexplored. One study reported an upregulation of Kv7.4 channel mRNA in VSMCs after the treatment with pro-inflammatory molecule, lipopolysaccharide (LPS) [23]. However, to the best of our knowledge, the mechanistic understanding of the possible link between Kv7.4 channel activity/expression and vascular inflammation is yet to be established.

In this study, we examined the influence of Kv7.4 channel activity on TNFR1-NF-κB signaling and its contribution to vascular inflammation and the development of vascular diseases.

2. Materials and methods

2.1. Human subjects

The study was carried out in accordance with the ethical principles for medical research involving human subjects set out in the Helsinki Declaration, and was approved by the ethical committee at Hebei Medical University (Shijiazhuang, China).

Human aortic dissection tissues or control samples were obtained from 9 patients from the Second Hospital of Hebei Medical University (Shijiazhuang, China). Samples for immunohistochemical staining were processed for paraffin embedding and cut 7 μm thick. Each specimen was fixed with 4% paraformaldehyde for immunohistochemistry study. All patients or their relatives gave informed consent prior to their participation in the study.

2.2. Animals

The Kv7.4 knock-out (*Kcnq4*$^{-/-}$) mouse line with a deletion of *Kcnq4* exons 6–8 was kindly provided by Prof Thomas Jentsch (FMP, MDC, Berlin, Germany). Generation of mice with an altered KCNQ4 gene was as follows [24]. Genomic sequence was obtained from a mouse ES cell line (MPI-2, derived from a 129SvJ mouse strain). A fragment of genomic DNA was amplified using primers in introns 1 and 10 and was cloned in the pKO-V901 vector (Lexicon Genetics). A loxP site was inserted by PCR between exons 5 and 6, and a 'floxed' neomycin resistance (NEO) cassette between exons 8 and 9 by ligation into an *Eco*47III site. A diphtheria toxin A cassette was fused 5'. Sequenced constructs were electroporated into MPI2 ES cells. Clones having undergone homologous recombination were transfected with a plasmid expressing Cre-recombinase. Cells with an exclusive deletion of the NEO cassette were used to generate mice with 'floxed' and dominant negative alleles, and those with deleted exons 6–8 (leading to a frameshift) for the KO line. Cells were injected into C57BL/6 blastocysts that were implanted into foster mothers. The resulting chimeras were bred with C57BL/6 females. Heterozygous animals stemming from two different ES cell clones were inbred to yield mutant mice. Genotyping was performed using three-primers: Primer1: GAGCCCCCTTTCCAGACCCTAC; Primer2: AGCTGATCACCGCCTGGTACATCG; Primer3: AGGCTGGGCTGAGACTGAAT. Reaction products of 342 bp, 460 bp or both, represent the wild type, homozygous *Kcnq4*$^{-/-}$ or heterozygous *Kcnq4*$^{-/-}$ mice, respectively. The elimination of exons 6–8 yielded a non-functional protein and the identification of *Kcnq4*$^{-/-}$ mice was consistent with the previous reports (Fig. S1A-C).

All animals were housed at controlled temperature, humidity and lighting (12 h: 12 h light-dark cycle) and provided free access to food (provided by Experimental Animal Center of Hebei Province) and water ad libitum. At the age of 8-12 weeks, male *Kcnq4*$^{-/-}$ mice and their WT littermates were used for the experiments. Male Sprague-Dawley (SD) rats, aged 4 weeks, were obtained from the Experimental Animal Center of Hebei Medical University. All animal procedures conformed to the Guide for the Care and Use of Laboratory Animals published by the US National Institutes of Health (NIH Publication, 8th Edition, 2011), and were approved by the Institutional Animal Care and Use Committee of Hebei Medical University.

2.3. Induction of intimal hyperplasia by the carotid artery ligation

Initial hyperplasia model induced by carotid artery ligation was generated as described previously [25]. Briefly, 8-12-week-old male mice were anesthetized with 1.5% isoflurane gas. The left common carotid artery was dissected and ligated near the carotid bifurcation using a 6-0 suture. In sham (unligated) animals, the suture was passed under the exposed left carotid artery but not tightened. At 14 days after surgery, all animals were anesthetized and perfused with cold PBS, and tissues were harvested for the experiments.

2.4. Mouse AAA models

For Ang II-Induced AAA formation, osmotic minipumps (Alzet, model 2004) were filled with saline or Angiotensin (Ang) II (A9525, Sigma Aldrich) at a dosage of 1,000 ng/kg/min dissolved in saline [26]. Mice were anesthetized with 1.5% isoflurane gas, and the pumps were implanted into the subcutaneous dorsum of the neck for 4 weeks. In vivo aortic ultrasound imaging was performed using the Vevo 770 ultrasound system (Visualsonics, Toronto, Canada) to confirm aortic aneurism development at day 28 after implantation. At day 28, mice were sacrificed, maximal diameters of aortas were photographed and the aortic diameters were measured *ex vivo*. The suprarenal aortas were identified between the last pair of intercostal arteries and the right renal branch. The maximum outer width of the abdominal aortas was analyzed using Image-Pro Plus software. AAA was defined as a localized dilation of

aorta greater than 50% of its adjacent intact portion.

$CaPO_4$-Induced AAA Model was performed as described previously [27]. Briefly, mice were anesthetized with 1.5% isoflurane gas. The infrarenal region of the abdominal aorta was isolated. A small piece of gauze soaked in 0.5 M $CaPO_4$ was applied perivascular for 15 minutes. The gauze was then replaced with another piece of phosphate buffered saline (PBS)-soaked gauze for 5 minutes. PBS was used for a sham operation in control mice. Mice were euthanized at 14 days after $CaPO_4$ stimulation, and their aortas were harvested for the analysis of gene expression and morphology.

2.5. Histological analyses

The animals were euthanized by an intraperitoneal injection of pentobarbital (80 mg/kg). Aortic samples were harvested, fixed in 4% PFA and imbedded in OCT. All sections were cut 5 μm thick for further studies. Aortic segments were stained with hematoxylin and eosin (H&E) or elastin van Gieson (EVG), (BASO Precision Optics Ltd.), according to the manufacturer's protocol for elastin assessment. The cross-sectional areas of the intima and media were measured in H&E-stained sections in a blinded manner by a single observer using Image Pro Plus 6.0 software (Media Cybernetics). A mean value was determined from at least four sections for each animal. Neointima formation was determined as the ratio of the intimal area to the medial area (I/M) [19].

Immunofluorescence staining was performed on acetone-fixed arterial sections of 5 μm thick sections. Sections were blocked using 10% normal goat serum in PBS for 30 min and incubated with primary antibodies against MMP-2 (1:50, Santa cruz), MMP-9 (1:50, Santa cruz), ICAM-1 (1:100, Abcam), collagenI, III (1:50, Abcam), NF-κB p65 (1:100, GeneTex), TNFR1 (1:50, Proteintech), TRADD (1:50, Proteintech), Kv7.4 (1:80, Alomone), SM22α (1:100, Proteintech), CD31 (1:100, BD Biosciences), FSP1 (1:100, Proteintech), at 4°C overnight. After washing 3 times with PBS sections were incubated with fluorescein-conjugated secondary antibodies (Alexa Fluor® 555 or Alexa Fluor 649, 1:200, Invitrogen) for 1 h at room temperature.

Nuclei were detected by DAPI (Antifade Mountant with DAPI, Thermofisher), images were captured by Leica TCS SP5 confocal microscope (Leica, Germany). For immunohistochemical staining, arterial sections were permeabilized with 0.1%Triton-X for 10 minutes, blocking with 10% normal goat serum in PBS for 30 min at room temperature. Primary antibodies against Kv7.4 (1:80, Alomone), NADPH oxidase (NOX) 2 (1:100, Abcam), NOX4 (1:100, Abcam) were incubated overnight at 4°C, followed by secondary antibody before staining with DAB Kit (ZSGB-BIO, Beijing, China). Nuclei were counterstained with hematoxylin.

2.6. Apoptosis assay

The apoptosis of VSMCs in the aorta of AngII-treated *Kcnq4*$^{-/-}$ mice and WT mice were detected using an ApopTag® Peroxidase In Situ Apoptosis Detection Kit (Sigma-Aldrich) according to the instructions. The terminal deoxynucleotidyl transferase dUTP nick end labeling (TUNEL) staining was imaged under inverted biological microscope (Leica).

2.7 Cell culture and treatment

VSMCs were isolated from the aortas of 60–80 g male SD rats anesthetized intraperitoneally with urethane, and cultured in low glucose DMEM (Invitrogen) supplemented with 10% FBS (Gibco), 100 U/mL penicillin, and 100 μg/mL streptomycin. Mouse VSMCs were isolated from the thoracic aorta of WT and *Kcnq4*$^{-/-}$ mouse, and grown in low glucose DMEM with 20% FBS. The VSMCs were maintained at 37°C in a humidified incubator equilibrated with 95%O_2/5% CO_2 gas mixture; cells were passaged 3-5 times before being used in the experiments. Mouse lung endothelial cells (mECs) were obtained from ATCC and maintained in Endothelial Cell Medium (ScienCell, no. 1001). Raw 264.7 cells were purchased from ATCC (TIB-71™), and cultured in low-glucose DMEM containing 10% FBS. Before stimulation with TNFα (20 ng/mL, PeproTech), VSMCs were incubated in serum-free medium for 24 h. For pharmacological studies, cells were pretreated for 12 h with the Kv7 channel blocker XE991 (3 μM), before the addition of TNF-α.

2.8. Analysis of microarray data

Samples of left carotid artery from the wild type (WT) and *Kcnq4*$^{-/-}$mice were obtained 14 days after partial ligation of the left carotid artery. Total RNA was extracted by using TRIzol® extraction method and a NucleoSpin RNA II kit (Macherey Nagel, Duren, Germany). Differentially expressed genes with statistical significance were identified through Volcano Plot filtering. GO, PANTHER and KEGG Analysis was applied to determine the roles of these differentially expressed genes played in these biological GO terms. All of the above steps were performed by the Shanghai Biotechnology Corporation.

2.9. Western blot and co-immunoprecipitation analysis

VSMCs were lysed in RIPA buffer (10 mM HEPES, pH 7.8, 10 mM KCl, 0.1 mM EDTA, 1 mM DTT, 0.5% NP-40 and 0.5 mM PMSF) and prepared for the extraction of whole cell protein samples. Equal amounts of protein were separated by 10% SDS-PAGE, and transferred to PVDF membrane. Membranes were blocked with 5% BSA (bovine serum albumin) for 1 hour at room temperature, and incubated with specific antibodies against MMP2 (1:500, Proteintech), MMP9 (1:500, Proteintech), ICAM-1 (1:500, Abcam), NF-κB p65 (1:500, GeneTex), TNFR1 (1:100, Proteintech), TRADD (1:100, Proteintech), IκBα (1:500, CST), *p*-IκBα (1:500, CST), Kv7.4 (1:500, Alomone), NOX2 (1:500, Abcam), NOX4 (1:500, Abcam) overnight, and then with HRP-conjugated secondary antibody (1: 20000, Abcam) for 1 hours. The blots were evaluated with GE ImageQuant™ LAS 4000 detection system. These experiments were replicated three times.

The total protein was extracted after stimulation, and then subjected to immunoprecipitation using anti-TNFR1, anti-TRADD at 4 °C for 4 h. Subsequently, the immune complexes were incubated with Protein A/G PLUS Agarose beads (Santa Cruz) in rotation at 4°C overnight. The immunoprecipitated molecules were analyzed by Western blot as described above.

2.10. Quantitative real-time PCR (qRT-PCR)

Total RNAs of the cells and tissues was extracted using TRIzol Reagent (Life Technologies). To test the amount of mRNA, cDNAs were synthesized using the M-MLV First Strand Kit (Life Technologies), and quantitative PCR was performed using SYBR Green qPCR SuperMix-UDG (Life Technologies). The sequence of the primers used for qRT-PCR of *Kcnq4* was 5'-ATGGGGCGCGTAGTCAAGGT-3' (sense); 5'- GGGCTGTGGTAGTCCGAGGTG -3' (antisense). For quantification, all RNA expression was normalized to the amount of GAPDH using the $2^{-\Delta\Delta Ct}$ method. These experiments were replicated three times.

2.11. Small interfering RNA (siRNA) transfection

Cultured VSMCs were grown to 50–60% confluence and then transfected with specific duplex siRNAs. *Kcnq4* siRNA (si*Kcnq4*), 5'-CCUUACUGGGCAU CUCCUUTT-3' and 5'-AAGGAGAUGCCCAGUAAGGTT-3. Scrambled siRNA (siCon) 5'-UCUCCGAACGUGUCACGUT-3' and 5'-ACGUGACACGUUCGGA GAATT-3' served as a negative control. The siRNAs were transiently transfected into VSMCs using RNAi-MAX reagent (Invitrogen). Eight hours after transfection, VSMCs were stimulated with TNF-α.

2.12. Plasmids construction and transfection

Mouse *Kcnq4* and its control cDNA were synthesized by Sangon Biotech (Shanghai, China) and cloned into pEGFP vector (Geneseed Biotech, Guangzhou, China). All of these clones were verified by sequencing. Transient transfection was carried out using Lipofectamine iMax Reagent (Invitrogen) according to manufacturer's protocol. 2.5-5 μg of plasmid DNA was used per transfection reaction.

2.13. Viral gene delivery

For SMC-specific *Kcnq4* deletion, the AAV-shRNA-*Kcnq4* was constructed and packaged by Hanbio (Shanghai, China) [28,29]. Specific shRNA against Kv7.4 with a SM22α promoter and non-targeting control shRNA were separately constructed in the same vector, and AAV serotype 9 viral particles harboring these sequences were generated by Hanbio (Shanghai, China). Mice were injected one of the above viral

particles (5×10^9 pfu/kg). After 30 days, the mice were randomly grouped and treated with carotid artery ligation as the above mentioned.

2.14. Drug administration

Kv7/M channel inhibitor XE991 was purchased from Sigma (St Louis, MO, USA) and dissolved in saline (0.9% NaCl). Mice were intraperitoneally injected with XE991 at a dose of 5 mg/kg/d for 14 days after $CaPO_4$-induced AAA surgery or carotid artery ligation.

2.15. Flow cytometry

Cells collected from mice ligated carotid arteries were isolated and blocked with anti-CD68 and anti-CD45 antibody for 30 min on ice. Surface markers were then stained for 30 min on ice and fixed and permeablized by Intracellular Fixation & Permeablization buffer set (BD), followed by intracellular antigen staining. Fluorescence labeled cells analyzed was performed using guava EasyCyte system (Merck), and FlowJo V10 software was used for data analysis and quantification.

2.15. Statistical analysis

All statistical analyses were performed with the SPSS 21.0 software. Data are presented as means ± standard deviation (SEM) from at least three independent experiments, and each independent experiment was repeated at least three times to obtain the mean. Two-group comparisons were analyzed by the Student’s t-test. For multiple comparisons or repeated measurements, ANOVA or repeated-measures ANOVA followed by Tukey's posthoc test was used. For all statistical comparisons, $P<0.05$ was considered significant. Fisher’s exact test was applied to the comparisons of AAA incidence and log-rank (Mantel-Cox) test was used for survival comparison between groups.

3. Results

3.1. Genetic deletion of Kv7.4 channel alleviates vascular lesions in mice

Pathological vascular remodeling is a hallmark of most vascular disorders such as atherosclerosis, postangioplasty restenosis, and aortic aneurysm; all of these disorders have a chronic inflammatory component. To investigate the correlation between Kv7.4 expression and vascular remodeling in response to injury, we initially prepared the neointimal hyperplasia model induced by the carotid artery ligation in mice. Immunohistochemical staining showed that the level of Kv7.4 expression was significantly increased in the neointimal region at 14 days after the ligation compared to the sham control (Fig. S1D). We next tested whether Kv7.4 channel expression also increases during the formation of abdominal aortic aneurysm (AAA), a condition that is characterized by degeneration of the elastic media and loss of VSMCs. To this end, mice were infused with AngII (1000 ng/kg/min) for 28 days. The AAA vessels displayed strongly increased Kv7.4 protein levels compared to the saline group (Fig. S1E). We further examined the expression of Kv7.4 in dissected human aortic aneurysms, and showed that the level of Kv7.4 expression within the lesion was significantly higher than that of normal arteries (Fig. S1F). Overall, these data indicate that Kv7.4 channel is upregulated during vascular remodeling, which is a common feature of arterial restenosis and aneurysm.

To further explore the role of Kv7.4 channel in vascular remodeling, we compared severity of vascular lesion between wild type (WT) and *Kcnq4*$^{-/-}$ mice using the models of both neointimal hyperplasia and AAA, respectively. The expression of Kv7.4 at mRNA and protein levels was increased in the neointimal formation of WT mice, compared with the sham group. However, the slight expression of Kv7.4 at mRNA and protein levels was observed in the normal vessels of *Kcnq4*$^{-/-}$ mice and not affected by the injury (Fig. S1G-J). Intriguingly, injury-induced neointimal hyperplasia was significantly ameliorated in the *Kcnq4*$^{-/-}$ mice (Fig. 1A). Accordingly, the ratio of I/M was also significantly reduced in the *Kcnq4*$^{-/-}$ mice compared to WT control (Fig. 1B). Consistently, the number of SM22α positive VSMCs was less in the neointima of *Kcnq4*$^{-/-}$ mice than that of WT mice (Fig. S1K, L), indicating a reduced proliferative activity. These findings suggest that Kv7.4 may promote neointimal formation in response to injury.

We further tested the effects of Kv7.4 deletion on AAA formation using AngII- and $CaPO_4$-induced AAA models. After Ang II infusion for 28 days, WT mice showed 27.0% (6/22) incidence of AAAs whereas there was no AAA formation in *Kcnq4*$^{-/-}$ mice (Fig. 1C, D). Accordingly, WT mice displayed increased maximal abdominal aortic diameter (1.10 ± 0.2 mm in AngII-injected mice vs. 0.58 ± 0.1 mm in the saline-injected controls, $P<0.05$). Yet, AngII produced no significant change in *Kcnq4*$^{-/-}$ mice (0.65 ± 0.16 mm in AngII-injected mice vs. 0.57 ± 0.12 mm in the saline controls, $P<0.05$; Fig. 1E, F). Pathologically, the degradation of elastin and collagen was obvious in the abdominal aortic wall of WT mice, but undetectable in *Kcnq4*$^{-/-}$ mice under AngII infusion (Fig. S2A, C-F). Furthermore, 13.6% (3/22) of WT mice died due to aortic rupture, while all *Kcnq4*$^{-/-}$ mice survived the procedure (Fig. S2B). Notably, the activity of VSMC apoptosis was increased in AngII-induced AAA model of *Kcnq4*$^{-/-}$ and WT mice (Fig. S2G). However, this increase was lower in the aorta of *Kcnq4*$^{-/-}$ mice than that of WT mice under the same conditions (Fig.S2H).

In $CaPO_4$-induced AAA model, WT mice showed 69% (9/13) incidence of AAAs (Fig. 1H), along with increased maximal abdominal aortic diameter (0.72 ± 0.05 mm in saline controls vs. 1.6 ± 0.11 mm in $CaPO_4$-treated WT mice, $P<0.05$; Fig 1J). In contrast, there was only 14% (2/14) incidence of AAA formation in *Kcnq4*$^{-/-}$ mice and only a modest increase of abdominal aortic diameter (0.67 ± 0.08mm in saline controls vs. 1.0 ± 0.02 mm in $CaPO_4$-treated *Kcnq4*$^{-/-}$ mice, $P<0.05$ as from the $CaPO_4$-treated *Kcnq4*$^{-/-}$ mice displayed intact internal elastic laminae compared to WT mice that exhibited the dilated infrarenal aortas and the elastic lamina degeneration (Fig. 1G, I). Taken together, these data suggest that impaired Kv7.4 inhibits AAA formation.

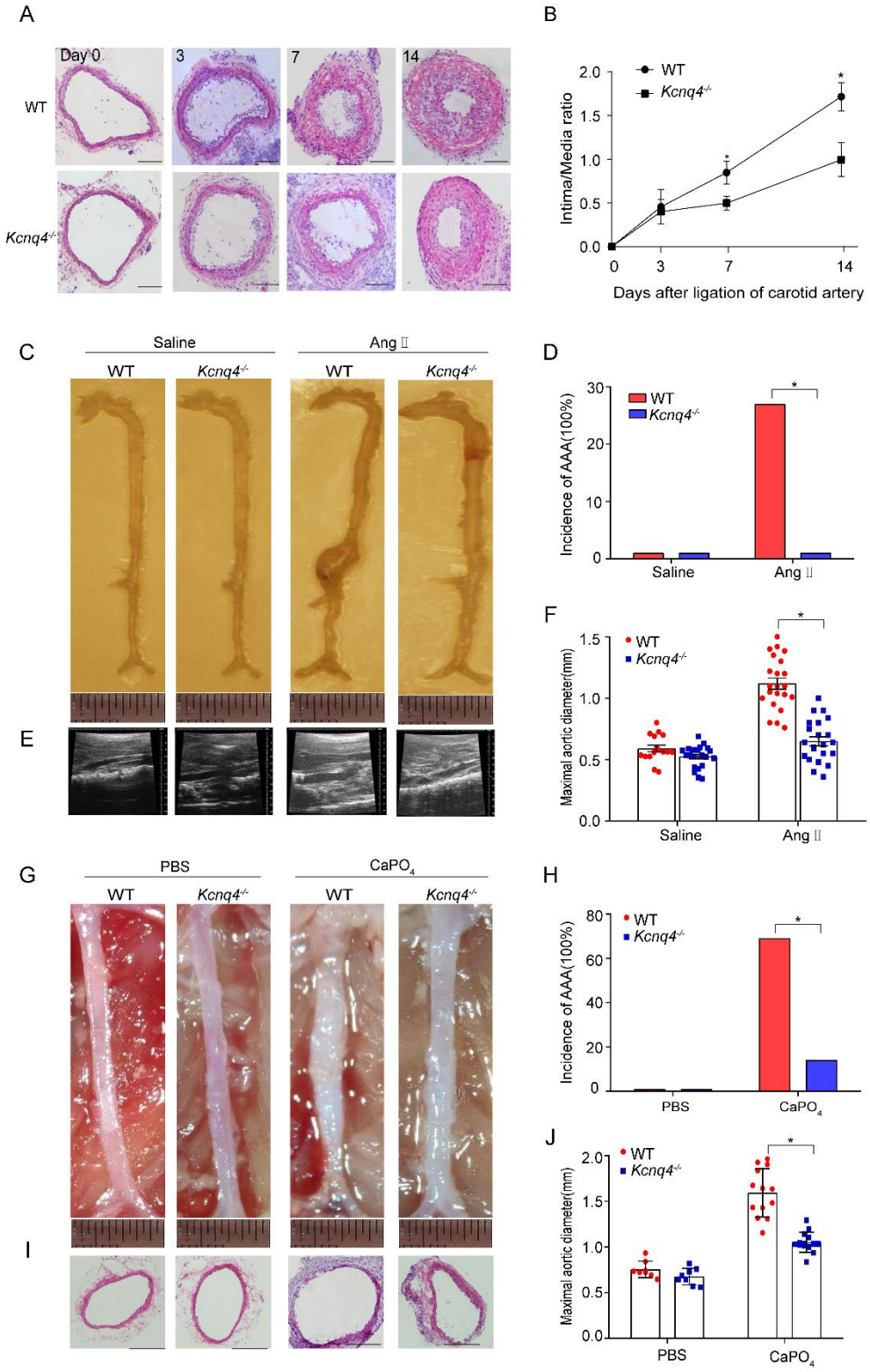

Figure 1. Vascular lesion is alleviated in vascular injury models of *Kcnq4*$^{-/-}$ mice. WT and *Kcnq4*$^{-/-}$ male mice (8-12 weeks) were used for the experiments**. (A, B)** The carotid arteries of mice were ligated for 0, 3, 7, 14 days. Hematoxylin and eosin (HE)

staining of representative cross sections in the ligated carotid arteries at different days (**A)**. Bar=200 μm, n=7 for each time point. The ratio of intimal/medial area (I/M ratio) over time (n=7) (**B)**. (**C-F)** Mice were infused with saline or AngII (1000 ng/kg/min) via subcutaneous osmotic minipumps for 4 weeks. Representative photographs showing the macroscopic features of aortas from saline- or AngII-infused WT and *Kcnq4*$^{-/-}$ male mice (**C**). Incidence of AAA in WT and *Kcnq4*$^{-/-}$ mice (**D**). Representative ultrasonography of the luminal diameters of abdominal aortic from saline- or Ang II-infused mice (**E)**. Quantification of maximal suprarenal abdominal aortic diameters measured *ex vivo* from saline- or AngII-infused WT and *Kcnq4*$^{-/-}$ mice (**F).** WT + saline, n=16; *Kcnq4*$^{-/-}$ + saline, n=22; WT + AngII, n=22; *Kcnq4*$^{-/-}$ + AngII, n=22. (**G-J)** Infrarenal aortic aneurysm of 8-12 weeks WT and *Kcnq4*$^{-/-}$ male mice was induced by $CaPO_4$ (0.5M) for 14 days. Representative morphology of infrarenal aortas dilation from WT and *Kcnq4*$^{-/-}$ mice exposed to saline or $CaPO_4$ for 14 days(**G)**. Incidence of AAA in WT and *Kcnq4*$^{-/-}$ mice by Chi-square test (**H)**. Representative staining of HE for the infrarenal aortas dilation of WT and *Kcnq4*$^{-/-}$ mice (**I**). Quantification of mean infrarenal aortas dilation from WT and *Kcnq4*$^{-/-}$ mice exposed to saline or $CaPO_4$ for 14 days (**J**). *P<0.05. WT+ saline, n=8; *Kcnq4*$^{-/-}$ + saline, n=8; WT+ $CaPO_4$, n=13; *Kcnq4*$^{-/-}$ + $CaPO_4$, n=14.

3.2 Kv7.4 deletion alters the profile of gene expression in neointimal hyperplasia

To reveal the potential role of Kv7.4 channel in vascular remodeling, we compared gene expression profiles of the normal arteries and neointimal hyperplasia in WT and *Kcnq4*$^{-/-}$ mice by microarray analysis. Twenty-two thousand five hundred sixty-four mRNAs were detected in four groups. The number and distribution of putative differentially expressed genes generated by microarray analysis were identified (2 fold change cut-off, p<0.05) by volcano plot (Fig. S3A). Using these criteria, there were a total of 110 genes differentially expressed in the normal arteries between *Kcnq4*$^{-/-}$ and WT mice. Furthermore, we also identified 381 differentially expressed genes in the neointimal hyperplasia of the two groups (Fig. S3A). To verify

the microarray data, we randomly selected 10 genes with different expression patterns and known vascular functions for qRT-PCR verification, and obtained similar expression profiles to the microarray data for the normal (Fig. S3B) and neointimal (Fig. S3C) arteries.

In the neointima between *Kcnq4*$^{-/-}$ and WT mice, the differentially expressed genes in biological process of GO terms were mainly related to response to stimulus, immune response and cell communication. Gene set enrichment analysis further identified top-ranked gene sets of immune system process and the cell surface receptor signaling pathways (Fig. S3D). Furthermore, protein classification of differentially expressed genes using PANTHER (protein analysis through evolutionary relationships) identified defense/immunity proteins involved in the neointima, which were reciprocally regulated by the neointimal hyperplasia in WT and *Kcnq4*$^{-/-}$ mice (Fig. S3E). Importantly, immune database (InnateDB) together with the R language analysis identified the following vascular inflammation-related genes: MMP2, MMP9 and ICAM-1, as being significantly downregulated in both, unligated and ligated arteries of *Kcnq4*$^{-/-}$ mice compared with WT mice (Fig. 2A, B). Additionally, representative pathways in KEGG for the neointima were associated with chemokines, cytokines and receptor-related pathways (Fig. 2C). Taken together, these data suggest that Kv7.4 is an important factor in vascular response to injury.

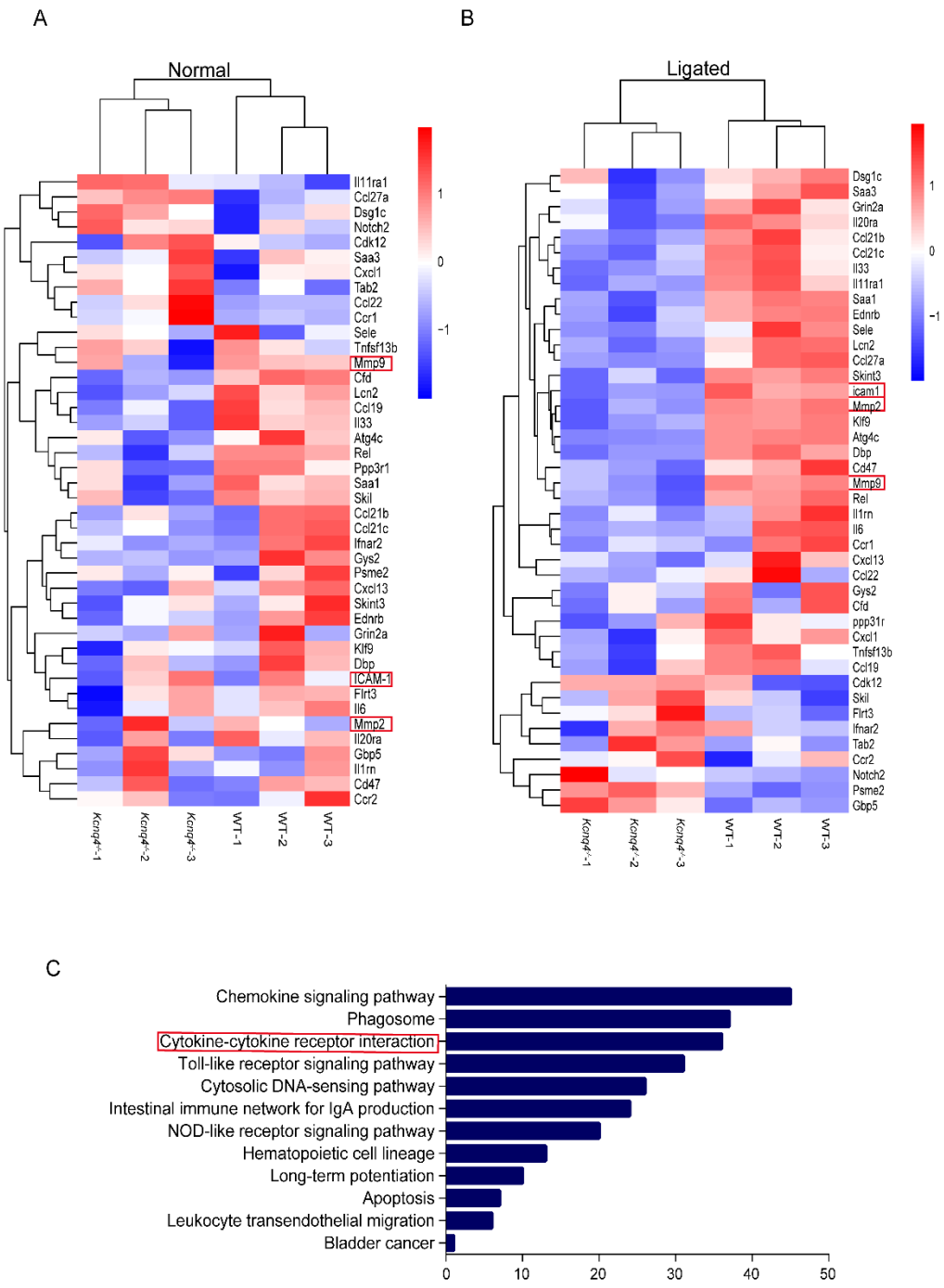

Figure 2. Inflammatory transcriptional program is ameliorated in the artery of *Kcnq4*$^{-/-}$ mice. Expression profile of mRNAs detected by microarray in arteries WT and *Kcnq4*$^{-/-}$ mice from either control or carotid artery ligated groups. **(A, B)** R analysis and Heat Map showed relative expression of inflammation-related genes in normal groups and carotid artery ligated groups of WT and *Kcnq4*$^{-/-}$ mice. **(C)** Pathway-analysis was performed using KEGG shows that differentially expressed

genes were mainly concentrated in chemokines, cytokines and receptor-related pathways in ligated groups. (n=3 per group).

3.3 Kv7.4 deletion ameliorates vascular inflammation and oxidative stress in response to injury

Inflammation is central to the pathophysiology of vascular remodeling in neointimal hyperplasia and AAA formation. MMP2/MMP9 play a key role in vascular remodeling through degrading collagen and extracellular matrix proteins and ICAM-1 stimulates the recruitment of inflammatory cells inside the vessels. Prompted by the results of the microarray analysis, we investigated whether Kv7.4 may play a key role in vascular inflammation. First, we determined the effect of Kv7.4 deletion on vascular inflammation induced by injury using the carotid artery ligation model. As expected, carotid artery ligation produced massive upregulation of all three pro-inflammatory cytokines, MMP2, MMP9, and ICAM-1 in the WT animals but this upregulation was reduced in the neointima of *Kcnq4*$^{-/-}$ mice (Fig. 3A, B), consistent with reduced I/M ratio in the knockout (Fig. 1B). To examine the infiltration of immune cells in the ligated carotid arteries of WT and *Kcnq4*$^{-/-}$ mice, we performed the analysis for monocytes/macrophages (CD68^{+}) and leukocytes (CD45^{+}) by flow cytometry and showed that the infiltration of monocytes/macrophages and leukocytes in the neointimal formation was not significant different between WT and *Kcnq4*$^{-/-}$ mice (Fig.S4A).

Next, we examined the expression of these pro-inflammatory molecules in AAA formation of *Kcnq4*$^{-/-}$mice treated with Ang II or $CaPO_4$. As was the case with the carotid artery ligation, AAA development was accompanied by marked increase in the MMP2, MMP9 and ICAM-1 expression in WT mice, but this was not observed in *Kcnq4*$^{-/-}$ mice in both AngII- and $CaPO_4$ –induced AAA models (Fig. 3C-F).

Oxidative stress has been implicated in chronic inflammation. NADPH oxidase (NOX)2 and NOX4 have emerged as a major initiating source for increased ROS

production in cardiovascular diseases [30]. To validate the role of oxidative stress in Kv7.4 induced inflammation, we examined the effects of Kv7.4 on NOX2 and NOX4 expression *in vivo* and *in vitro*. Immunohistochemical staining and Western blot showed that the expression of NOX2 and NOX4 was no difference in the vessel wall between WT and *Kcnq4*$^{-/-}$ mice under basal conditions, and was increased in AngII-induced AAA formation of WT mice (Fig. 3G-J, S4B-E). However, this increase was significantly reduced in *Kcnq4*$^{-/-}$ mice under the same conditions. Furthermore, TNFα treatment upregulated the expression of NOX2 and NOX4 in WT VSMCs, which was abolished *Kcnq4*$^{-/-}$ VSMCs under the same conditions (Fig. 3K, L), indicating that inflammation and oxidative stress are both involved in Kv7.4-induced vascular remodeling. Overall, these findings suggest that Kv7.4 may be a component of the vascular inflammatory response to injury, which is critical for the development of restenosis or AAA onset under pro-inflammatory cues.

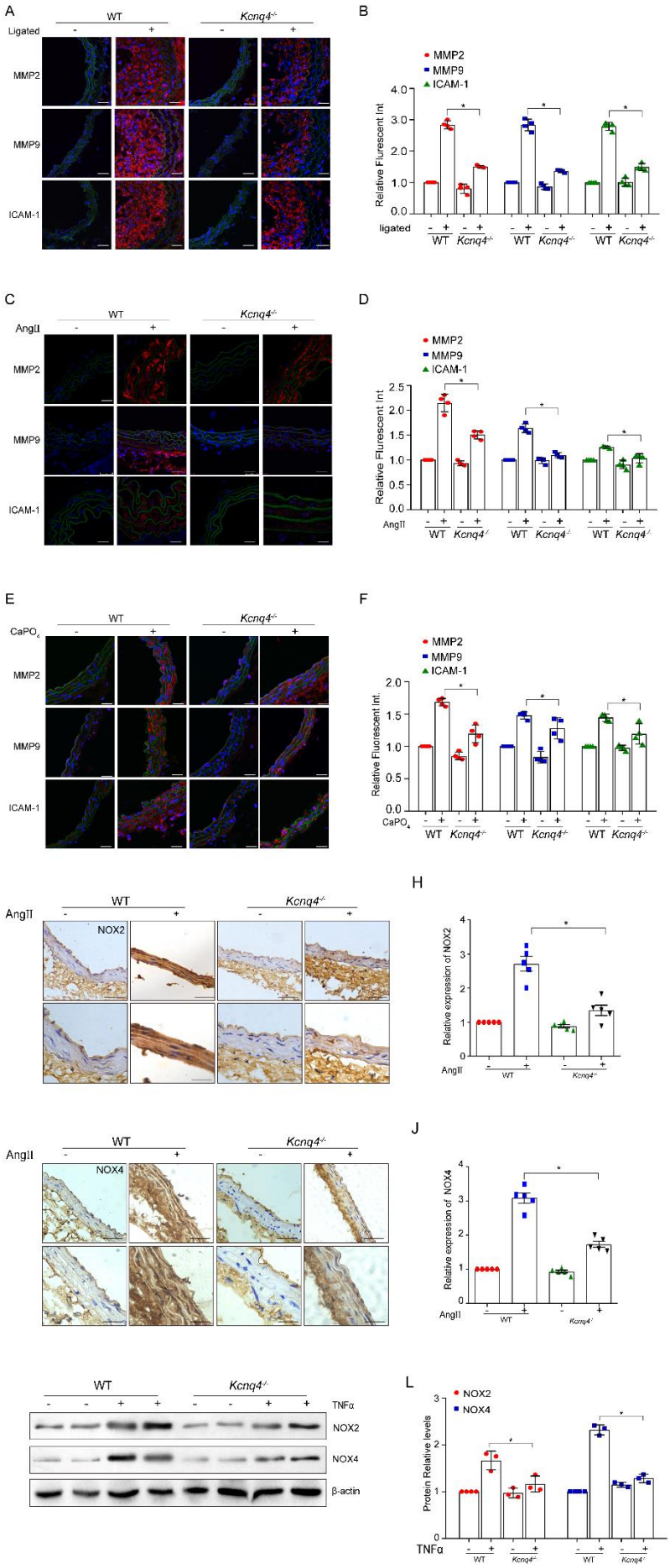
A
WT
Kcnq4-/-
Ligated
MMP2
MMP9
ICAM-1
B
MMP2
MMP9
ICAM-1
Relative Fluorescent Int.
ligated
C
AngII
D
E
CaPO4
F
G
NOX2
Relative expression of NOX2
H
I
NOX4
Relative expression of NOX4
J
K
TNFα
β-actin
L
Protein Relative levels

Figure 3. Kv7.4 deletion ameliorates vascular inflammation and oxidative stress in response to injury. (A) Representative immunofluorescence staining with proinflammatory cytokines, MMP2, MMP9 and ICAM-1 (all in red) in the neointima from the WT or *Kcnq4*$^{-/-}$ mice at 14 days after carotid artery ligation, bars=25 μm. The green fluorescence is the autofluorescence of the elastic plate; blue staining is DAPI. **(B)** Fluorescence intensity from images as these shown in Aare summarized as mean ± SEM. n=4 per group, *P<0.05. **(C, D)** MMP2, MMP9 and ICAM-1staining was performed on infiltrative suprarenal abdominal aortas from saline- or Ang II-infused mice (either WT or *Kcnq4*$^{-/-}$), bars=25 μm; n=4 per group, *P<0.05. **(E, F)** MMP2, MMP9 and ICAM-1 staining was performed on aortic sections from $CaPO_4$-treated mice (either WT or *Kcnq4*$^{-/-}$), bars=25 μm; n=4 per group, *P<0.05. **(G, H)** Representative immunohistochemical staining of NOX2 in the aortas from saline- and Ang II-infused WT and *Kcnq4*$^{-/-}$ mice. Bar=100 μm (upper), Bar=50 μm (lower). Data are presented as mean ± SEM, n=5 per group, *P<0.05. **(I, J)** Representative immunohistochemical staining of NOX4 in the aortas from saline- and Ang II-infused WT and *Kcnq4*$^{-/-}$ mice. Bar=100 μm (upper), Bar=50 μm (lower). Data are presented as mean ± SEM, n=5 per group, *P<0.05. **(K, L)** Western blot analysis of the expression of NOX2 and NOX4 in VSMCs from WT or *Kcnq4*$^{-/-}$ mice stimulated with TNF-α for 24 hours. Data are summarized as mean ± SEM, n=3 per group, *P<0.05.

3.4. Kv7.4 deficiency in VSMCs prevents inflammatory response in vascular remodeling

To determine potential factors for suppressed vascular inflammation in *Kcnq4*$^{-/-}$ mice, the expression of Kv7.4 in vascular cells was tested, including mouse VSMCs, mouse lung endothelial cells (mECs) and macrophage line RAW264.7 cells. Western blot and qRT-PCR showed that Kv7.4 highly expressed in VSMCs, less abundant in mECs and even less so in RAW264.7 cells (Fig. 4A, B, S5A). Pro-inflammatory cytokine, TNFα induced strong upregulation of Kv7.4 mRNA and protein in VSMCs, the effect was less pronounced in mECs and not seen in RAW264.7 cells (Fig. 4C, D). The level of *Kcnq4* mRNA significantly increased in the VSMCs treated with TNFα

or LPS at different time points (Fig. S5B).

To further determine whether the expression of Kv7.4 is restricted to VSMCs or whether other cell types after injury, we performed the co-localization analysis for Kv7.4 and the cell type-specific markers in the tissue section of mouse AAA using immunofluorescence staining. The expression of Kv7.4 was higher in $SM22\alpha^+$ VSMCs than that in $CD31^+$ ECs and FSP^+ fibroblasts in AAA formation (Fig.S5C). However, little Kv7.4 expression were observed in $CD31^+$ ECs and FSP^+ fibroblasts after injury, indicating that the upregulation of Kv7.4 expression may be more prominent in VSMCs, compared to the other cell types in AAA formation. These findings suggest that Kv7.4 was highly expressed in VSMCs and actively participated in vascular remodeling after injury.

Importantly, knockdown of *Kcnq4* using the specific siRNA (Fig. 4E, F), or genetic deletion (Fig. 4G, H) of *Kcnq4* or pharmacological inhibition of Kv7 channels (XE991, 3 μM; Fig. S5D) suppressed the TNFα-induced upregulation of MMP2, MMP9 and ICAM-1 at both the protein and the mRNA levels in VSMCs. Notably, the TNFα-induced upregulation of the pro-inflammatory genes in the *Kcnq4*$^{-/-}$ mice was recovered by rescue of Kv7.4 expression in VSMCs infected by Ad-Kv7.4 (Fig. S5E).

To further investigate whether disruption of Kv7.4 expression in VSMCs prevents pathological vascular remodeling, we produced an AAV carrying shRNA against *Kcnq4* to specifically knockdown Kv7.4 expression in VSMCs in *vivo* [31] (Fig. S6A). As anticipated, knockdown yielded a significant inhibition of Kv7.4 expression specific to VSMCs, as ensured by using the AAV-shRNA which carried the VSMC special promoter [32] (Fig. 4I, J and Fig. S6B-D). In the next step, AAV-shKv7.4 mice received the carotid artery ligation for 14 days. There was a substantial decrease in the ratio of I/M in AAV-shKv7.4 mice compared with the scr-RNA group (Fig. 4 K and Fig. S6E). The mRNA level of MMP2, MMP9 and ICAM-1 were significantly suppressed in the ligated arteries of AAV-shKv7.4 group, compared to the scr-RNA control (Fig. 4L). Collectively, these data further support the importance of Kv7.4 in VSMCs for the inflammatory response in vascular remodeling induced by injury.

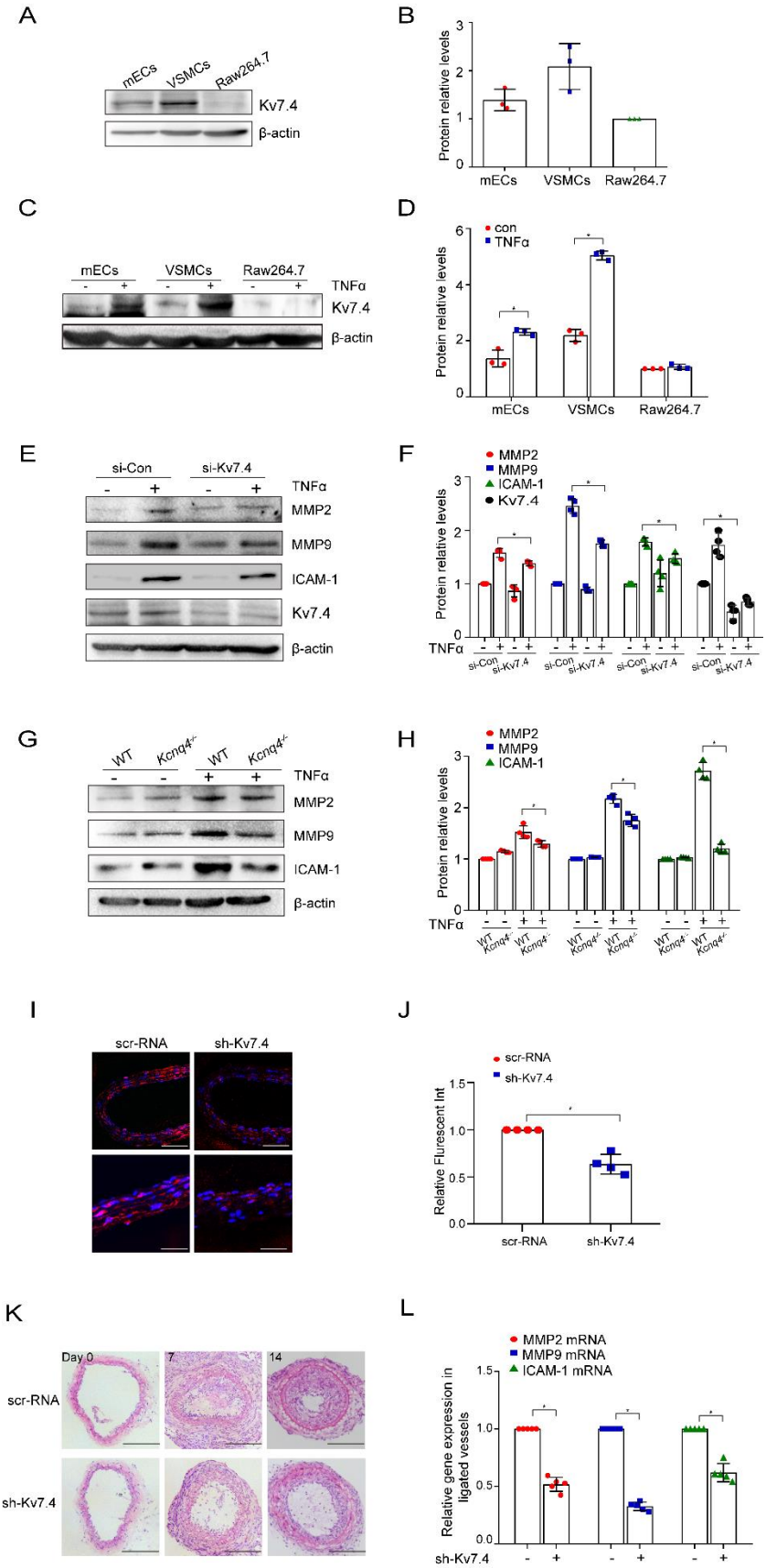
A
mECs
VSMCs
Raw264.7
Kv7.4
β-actin
B
Protein relative levels
mECs
VSMCs
Raw264.7
C
TNFα
D
con
TNFα
E
si-Con
si-Kv7.4
MMP2
MMP9
ICAM-1
F
G
WT
Kcnq4-/-
H
I
scr-RNA
sh-Kv7.4
J
Relative Flurescent Int
K
Day 0
7
14
L
MMP2 mRNA
MMP9 mRNA
ICAM-1 mRNA
Relative gene expression in ligated vessels

Figure 4. The role of Kv7.4 in inflammatory response in VSMCs. (A) Western blot was performed to detect Kv7.4 expression in Raw264.7 cells, VSMCs and mECs. (**B)** Protein content was analyzed by densitometry from experiments as these shown in (**A**) Data are summarized as mean ± SEM. n=3 per group, **P*<0.05. (**C)** Kv7.4 expression in Raw264.7 cells, VSMCs and mECs was detected by Western blot before and after TNFα (20 ng/ml) treatment 24 hours. (**D)** Protein content was analyzed by densitometry from experiments. Data are summarized as mean ± SEM. n=3 per group, *P<0.05. (**E)** VSMCs were transfected with non-targeting control siRNA (si-Con) or si-Kv7.4, and then were treated with TNFα for 24 hours. The expression of MMP2, MMP9 and ICAM-1 was detected by Western blot. (**F**) Protein content was analyzed by densitometry from experiments. Data are summarized as mean ± SEM. n=4 per group, *P<0.05. (**G)** The expression of MMP2, MMP9 and ICAM-1 in VSMCs from WT or *Kcnq4*$^{-/-}$ mice stimulated with TNFα for 24 hours was detected by Western blot. (**H)** Protein content was analyzed by densitometry from experiments. Data are summarized as mean ± SEM. n=4 per group, *P<0.05. (**I, J)** Representative immunofluorescence staining of Kv7.4 in the carotid arteries of mice infected with AAV-shKv7.4 and AAV-scrRNA. Bar=50 μm (upper), Bar=25 μm (lower). The red staining is Kv7.4. Fluorescence intensity from images was summarized as mean ± SEM. n=4 per group, *P<0.05. (**K)** Representative HE staining of the cross sections in the ligated carotid arteries at 7 and 14 days after VSMC-specific knockdown of *Kcnq4* using AAV-shKv7.4. Bar=200 μm. (**L)** qRT-PCR was conducted to detect MMP2, MMP9, and ICAM-1 mRNA in the ligated carotid artery of mice infected with AAV-shKv7.4 and AAV-scrRNA. Data are summarized as mean ± SEM. n=5 per group, *P<0.05.

3.5. Kv7.4 promotes TNFα-activated TNFR1-NF-κB signaling in VSMCs

To further probe the involvement of Kv7.4 with the inflammation signaling in the vasculature, we tested the effect of Kv7.4 activity on NF-κB activation. Pre-incubation of VSMCs with XE991 (3 μM) for 12 h inhibited TNFα-induced

nuclear translocation of NF-κB p65 (Fig. 5A), a result confirmed by Western blot (Fig. 5B). Accordingly, the TNFα-induced nuclear translocation of NF-κB was significantly reduced in *Kcnq4*$^{-/-}$ mice (Fig. 5A-B). Rescue of Kv7.4 expression by infection of VSMCs with Ad-Kv7.4 reinstated nuclear translocation of NF-κB p65 in *Kcnq4*$^{-/-}$ VSMCs in response to TNFα (Fig. 5A). To examine whether the arrest of nuclear translocation of NF-κB p65 existed in *Kcnq4*$^{-/-}$ mice *in vivo*, we performed immunofluorescence staining for the cross-sections of the carotid arteries of WT and *Kcnq4*$^{-/-}$ mice after ligation. The proportion of VSMCs displaying nuclear localization of NF-κB p65 was significantly reduced in injured arteries from *Kcnq4*$^{-/-}$ mice compared to WT control (Fig. S7A), suggesting that Kv7.4 contributes to activation of NF-κB *in vitro* and *in vivo*.

The IKK-mediated phosphorylation and subsequent IκBα degradation is the most important mechanism that leads to NF-κB activation via its subsequent dissociation from IκBα [33]. To determine if these steps are important for the role of Kv7.4 in promoting NF-κB nuclear translocation, we tested the phosphorylation and degradation of IκBα. The level of phosphorylated IκBα was significantly decreased and IκBα protein was significantly increased during TNFα treatment in VSMCs of *Kcnq4*$^{-/-}$ mice, as compared to WT control (Fig. 5C). Similar results were observed in the preincubation of VSMCs with XE991 (3 μM, 12 h) during TNFα treatment (Fig. S7B).

TNFα induces binding of TRADD to TNFR1 and subsequent activation of NF-κB [8]. In untreated VSMCs from WT and *Kcnq4*$^{-/-}$ mice, an even distribution of TNFR1 and TRADD in the cytoplasm was observed (Fig. 5D). After TNFα treatment, TNFR1 and TRADD shifted to a plasma membrane co-localization, as a punctate pattern of yellow color appeared at the edge of the cells. Interestingly, this co-localization was reduced in XE991-pretreated VSMCs from WT mice or in VSMCs from *Kcnq4*$^{-/-}$ mice (Fig. 5D). In the latter case, the interaction between TNFR1 and TRADD was rescued by the infection of Ad-Kv7.4 (Fig. 5D).

Next, we performed cross co-immunoprecipitation to directly examine the ability

of Kv7.4 to interfere with the formation of the TNFR1-TRADD complex in VSMCs isolated from *Kcnq4*$^{-/-}$ mice. TNFR1 was immunoprecipitated with anti-TRADD, and TRADD was also coimmunoprecipitated by anti-TNFR1 in WT VSMCs upon TNFα stimulation (Fig. 5E). TNFα-induced interaction between TNFR1 and TRADD was significantly reduced in *Kcnq4*$^{-/-}$ VSMCs. And overexpression of Kv7.4 in *Kcnq4*$^{-/-}$ VSMCs could significantly reverse the interaction between TNFR1 and TRADD (Fig. 5F). Taken together, these findings suggest that Kv7.4 channel promotes vascular inflammation by activation of TNFR1-TRADD-IκBα-NF-κB signaling pathway in VSMCs.

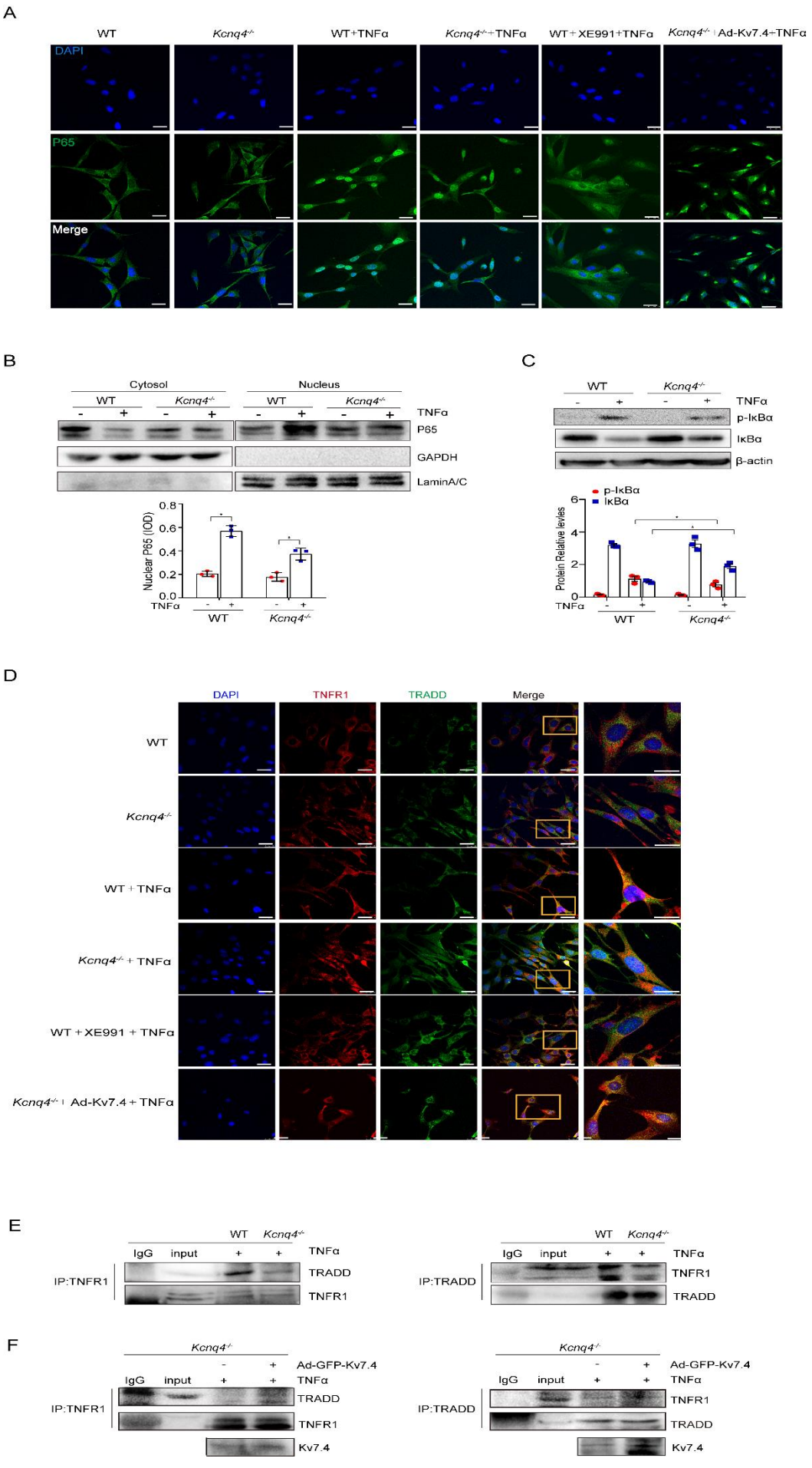
A
WT
Kcnq4-/-
WT+TNFα
Kcnq4-/-+TNFα
WT+XE991+TNFα
Kcnq4-/- | Ad-Kv7.4+TNFα
DAPI
P65
Merge
B
Cytosol
Nucleus
WT
Kcnq4-/-
TNFα
P65
GAPDH
LaminA/C
Nuclear P65 (IOD)
C
p-IκBα
IκBα
β-actin
Protein Relative levles
D
DAPI
TNFR1
TRADD
Merge
WT
Kcnq4-/-
WT + TNFα
Kcnq4-/- + TNFα
WT + XE991 + TNFα
Kcnq4-/- | Ad-Kv7.4 + TNFα
E
IgG
input
IP:TNFR1
IP:TRADD
F
Ad-GFP-Kv7.4
Kv7.4

Figure 5. Kv7.4 promotes TNFα-activated TNFR1-NF-κB signaling in VSMCs. **(A)** Representative images for immunofluorescence staining of NF-κB (P65) nuclear translocation in VSMCs of WT and *Kcnq4*$^{-/-}$ mice, preincubated with XE991 (3 μM) or transfected with Ad-GFP-Kv7.4 for 36 hours before stimulation with TNFα (20 ng/ml) for 30 minutes. Bars=25 μm. (**B)** Western blot for NF-κB (P65) in VSMCs of WT and *Kcnq4*$^{-/-}$ mice stimulated with TNFα for 30 minutes. Densitometry data are presented as the mean ± SEM in the bottom panel. n=3 per group, *P < 0.05. (**C)** Western blot for p-IκBα and IκBα in VSMCs of WT and *Kcnq4*$^{-/-}$ mice stimulated with TNFα for 10 minutes. Densitometry data are presented as the mean ± SEM in the bottom panel. n=3 per group, *P < 0.05. **(D)** Co-localization of TNFR1 and TRADD in VSMCs of WT and *Kcnq4*$^{-/-}$ mice, preincubated with XE991 (3 μM) or infected with Ad-Kv7.4 for 36 hours before stimulation with TNFα (20 ng/ml) for 10 minutes. Bars=25 μm. (**E**) Co-immunoprecipitation of TNFR1 and TRADD in VSMCs of WT and *Kcnq4*$^{-/-}$ mice stimulated with TNFα for 10 minutes. Left: Cell lysates were immunoprecipitated with anti-TNFR1 antibody. Right: Cell lysates were immunoprecipitated with anti-TRADD antibody. **(F)** Co-immunoprecipitation of TNFR1 and TRADD in VSMCs from *Kcnq4*$^{-/-}$ mice infected with Ad-Kv7.4. Cells were stimulated with TNFα for 10 minutes. Left: Cell lysates were immunoprecipitated with anti-TNFR1 antibody. Right: Cell lysates were immunoprecipitated with anti-TRADD antibody.

3.6 Pharmacological inhibition of Kv7.4 channels reduces vascular inflammation and vascular lesion *in vivo*

To further investigate whether acute pharmacological inhibition of Kv7.4 channels could present a therapeutic opportunity for treatment of vascular inflammatory disorders, we tested whether XE991 could prevent pathological vascular remodeling in mice with carotid artery ligation. Administration of XE991 (i.p. 5 mg/kg/d) next day after the surgical procedure in mice resulted in significant reduction of the ratio of I/M and MMP2, MMP9 and ICAM-1 mRNA level, as

compared to the saline control (Fig. 6A-C). Congruent results were obtained in the $CaPO_4$-induced AAA model, thus a significant decrease in incidence of AAA was observed in the XE991 group (28.6% or 2/7), compared to the saline control (66.7% or 6/9; $P<0.05$; Fig. 6E). The maximal abdominal aortic diameter was also reduced in the XE991 group (XE991 group, 1.17 ± 0.14 mm vs. saline group, 1.52 ± 0.09 mm; $P<0.05$; Fig. 6D, F), Furthermore, the expression of the pro-inflammatory cytokines was down-regulated in the XE991 group (Fig. 6G, H). These results suggested that acute pharmacological inhibition of Kv7.4 channel represents a plausible strategy to treat vascular inflammation disorders. It is important to note, that while both Kv7.4 and Kv7.5 are expressed in VSMCs, Kv7.5 is over 10 times less sensitive to XE991 as compared to Kv7.4 [17,34] and, thus, would be much less affected in our experimental conditions.

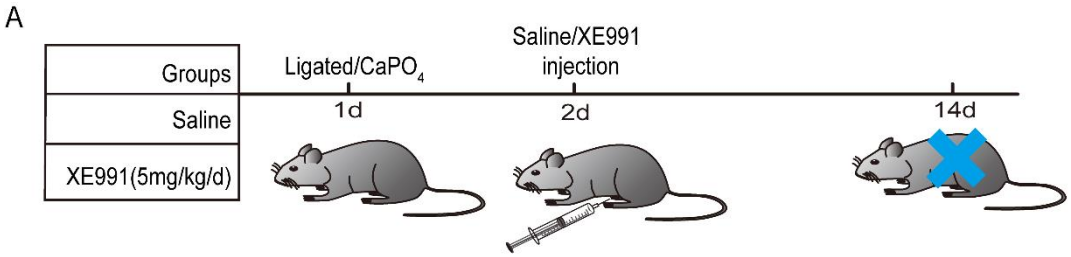
A
Groups
Saline
XE991(5mg/kg/d)
Ligated/CaPO4
1d
Saline/XE991
injection
2d
14d

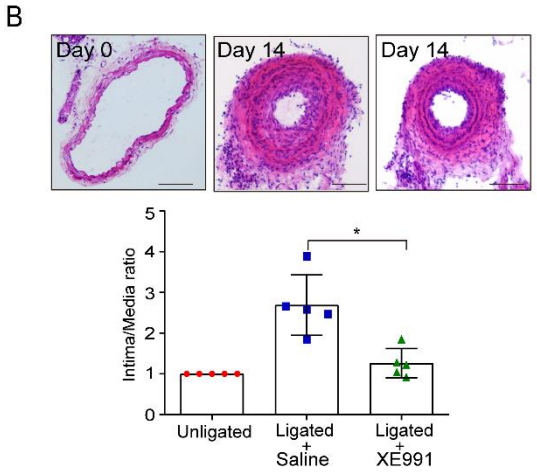
B
Day 0
Day 14
Day 14
Intima/Media ratio
Unligated
Ligated + Saline
Ligated + XE991

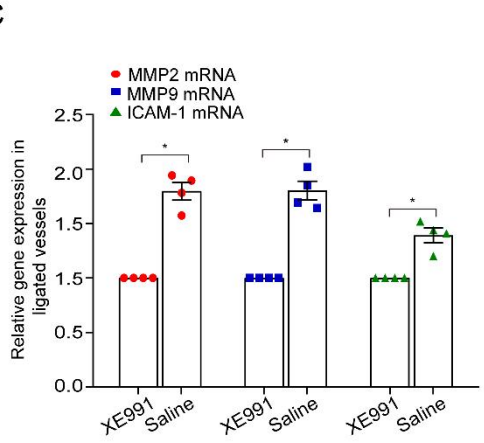
C
MMP2 mRNA
MMP9 mRNA
ICAM-1 mRNA
Relative gene expression in ligated vessels
XE991
Saline

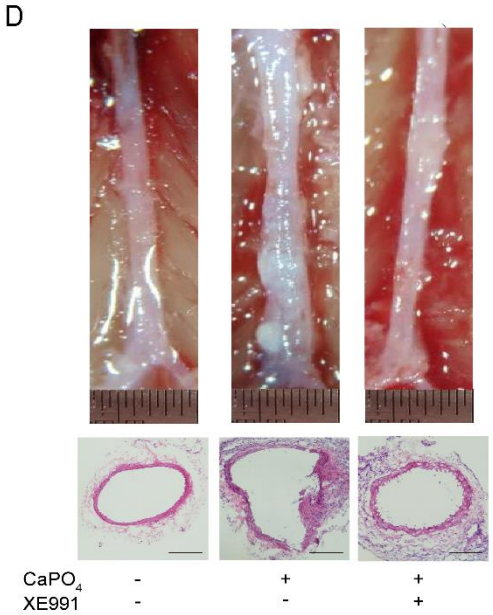
D
CaPO4
XE991

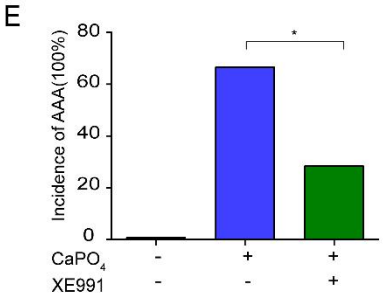
E
Incidence of AAA(100%)
CaPO4
XE991

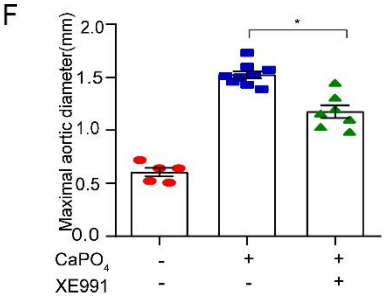
F
Maximal aortic diameter(mm)
CaPO4
XE991

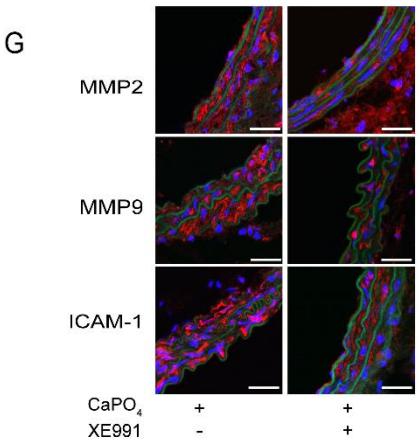
G
MMP2
MMP9
ICAM-1
CaPO4
XE991

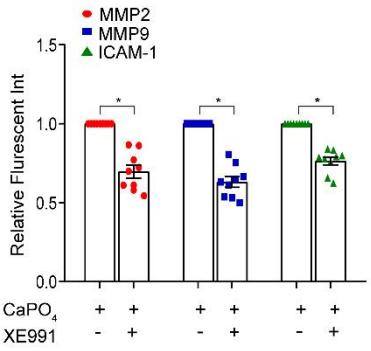
H
MMP2
MMP9
ICAM-1
Relative Flurescent Int
CaPO4
XE991

Figure 6. Inhibition of Kv7.4 reduces vascular inflammation and vascular lesion in mouse models. (**A)** Flow diagram of carotid artery ligation or treatment of $CaPO_4$ in mice, followed by with the i.p. injection of XE991 (3 μM). (**B)** Representative HE staining for the cross sections of the ligated carotid arteries with or without XE991 treatment. Bar=200 μm. The ratio of I/M was measured in the injured carotid arteries and presented as the mean ± SEM in the panel below. n=5 per group, *P < 0.05. (**C)** qRT-PCR was conducted to detect MMP2, MMP9, and ICAM-1 expression in carotid artery ligated mice. Data are summarized as mean ± SEM. n=4 per group, *P < 0.05. (**D)** Representative images showing aortas from animals stimulated with $CaPO_4$ with or without XE991 injection. Representative HE staining for the infrarenal aortas dilation induced with $CaPO_4$ in mice was shown in the lower panel. Bar=200 μm. (**E)** Incidence of AAA induced by $CaPO_4$ in mice with or without XE991 injection. (**F)** Maximal diameter in abdominal region from $CaPO_4$-treated mice with or without XE991 injection. Data are presented as the mean ± SEM. Sham group, n=5; $CaPO_4$ + saline, n=9; $CaPO_4$ + XE991, n=7, *P < 0.05. (**G, H)** Representative immunofluorescence staining of MMP2, MMP9 and ICAM-1 in aortic sections of $CaPO_4$-treated mice with or without XE991 injection. Data are presented as the mean ± SEM. n=9 per group, *P < 0.05.

4. Discussion

In this study, we demonstrated that Kv7.4 channel promotes vascular remodeling by enhancing expression of inflammatory molecules via the TNFR1-NF-κB signaling pathway in the vascular inflammatory disorders. Kv7.4 channel expression is induced in injured arteries and this increased expression promoted vascular remodeling and the development of neointimal hyperplasia and AAA. *Kcnq4* knockout, knockdown or Kv7 channel inhibition suppressed vascular inflammation, which was characterized by down-regulation of MMP2, MMP9 and ICAM-1 through inhibition of TNFR1-TRADD-IκBα-NF-κB signaling in VSMCs. In addition, we demonstrate that Kv7.4 inhibition represents a potential strategy to treat vascular inflammatory

disorders.

Adaptive alterations of the vessel wall architecture, called vascular remodeling, can be found in restenosis after vascular interventions [35-37], during the formation of aneurysms [38], in arterial hypertension [39,40], and in atherosclerosis [41,42]. We used neointimal hyperplasia and abdominal aortic aneurysm (AngII- and $CaPO_4$-induced) models of vascular remodeling to validate the role of Kv7.4 channels in this pathological process. We report the following main findings: 1) Kv7.4 channel is highly induced in neointimal formation and aortic dissecting aneurysm samples from human patients or mice. 2) In *Kcnq4*$^{-/-}$ mice, injury-induced neointimal hyperplasia and formation of AAA (as well as the expression of inflammatory markers of the above processes) was largely prevented; these effects were mimicked by transient Kv7.4 knockdown and rescued by re-expression of Kv7.4 channel. 3) Injury-induced neointimal hyperplasia and formation of AAA was suppressed by the treatment of Kv7/M channel inhibitor, XE991. Thus, these results pinpoint Kv7.4 channels as key determinants of the vascular remodeling.

Neointimal hyperplasia and AAA development are triggered by vascular inflammation, a process which disturbs normal signal transduction within vascular cells, changes the communication between vascular cells and causes remodeling of vascular wall [43]. We provide evidence that Kv7.4 channel expressed in VSMCs mediates inflammatory response which, in turn, contributes to vascular remodeling. The following findings support the above conclusion: 1) the levels of *Kcnq4* mRNA and Kv7.4 protein significantly increased in VSMCs treated with TNFα or LPS, compared to other cell types. 2) Heatmap representation of transcriptomic profiling showed that various vascular inflammation-related genes were significantly downregulated in the neointima arteries of *Kcnq4*$^{-/-}$ mice. 3) The increased expression of pro-inflammatory cytokines MMP-2/MMP-9 and ICAM-1 was reduced in the neointimal hyperplasia and AAA models of *Kcnq4*$^{-/-}$ mice. 4) TNFα-induced expression of MMP-2/MMP-9 and ICAM-1 in VSMCs was reduced by *Kcnq4* knockout or knockdown and by Kv7.4 channel inhibition. Endothelial cells have been found to trigger vascular remodeling by releasing proteases, or recruiting

macrophages along with other neutrophils, into the medial layer [44,45]. Our results showed the level of Kv7.4 channel expression in endothelial cells was lower, as compared to the VSMCs.

TNFα has an important role in VSMC communication system, and is involved in the early stages of the inflammatory response. The binding of TNFα to TNFR1 recruits RIP1 and TRAF2 to TRADD to form complex I, leading to activation of IKK complex, which is then followed by IκBα degradation and NF-κB nuclear translocation [8,9]. In the present study, we found that the TNFα-induced interaction between TNFR1 and TRADD, degradation of IκBα and nuclear translocation of NF-κB p65 were all reduced in the VSMCs from *Kcnq4*$^{-/-}$ mice or upon Kv7 channel inhibition in the VSMCs from the WT animals. Our study suggested that Kv7.4 promotes activation of TNFR1-TRADD-IκBα-NF-κB signaling in VSMCs. Inhibition of Kv7.4 suppresses the TNFα-induced TRADD-FADD interaction, thereby attenuating IκBα-NF-κB signaling cascades. Yet, the mechanism underlying Kv7.4 participation in the TNFα-induced TRADD-FADD interaction remains to be uncovered in future studies.

XE991, an inhibitor of the KCNQ2-3 channels, was studied initially in Alzheimer's disease by decreasing the stimulation threshold for certain cognitive processes and for long-term changes in synaptic efficacy and its enhancement of acetylcholine release in cholinergic nerve terminals in the brain [46]. In our study, we found that application of XE991 could inhibit injury-induced neointimal hyperplasia and formation of AAA. However, XE991 has several potential adverse reactions. XE991 can contribute to hypertension via enhance in vasoconstrictor responses [47], induce nociception in the model of injection of XE991 into rat paw [48], and exacerbate seizures [49]. Despite the potential side effects of Kv7 channel inhibitors, our study provides a new target for vascular inflammation.

In summary, we show that inhibition of Kv7.4 channel suppressed activation of TNFR1-NF-κB signaling in VSMCs which prevented vascular inflammation, specifically in vascular inflammation associated with neointimal hyperplasia and

AAA formation. Kv7.4 channel inhibitor might be considered as a potential target for future vascular inflammatory disease treatments.

However, several questions in understanding the function of Kv7.4 in vascular inflammation and vascular remodeling still remain to be clarified. First, Kv7.4 promotes vascular inflammation and oxidative stress in response to injury, whether Kv7.4 activating NF-κB induces oxidative stress, or the reverse, is unclear. Second, we have demonstrated that importance of Kv7.4 in VSMCs for the inflammatory response in vascular remodeling induced by injury, and nonetheless, contribution of endothelial Kv7.4 channel to inflammatory response in vascular remodeling cannot be ruled out at present, as Kv7.4 protein was up-regulated in the endothelial cells treated with TNFα. Third, a recent study demonstrated that cigarette smoke directly contributes to pulmonary arterial remodeling through diminished levels and function in the Kv7.4 channel [50], further investigation is required to determine whether Kv74 has conflicting effects on both the promotion and resolution of vascular remodeling in different vessel bed or under different conditions.

Acknowledgments

This work is supported by the National Natural Science Foundation of China (no. 91849102 to HM and 31872788 to FZ); Natural Science Foundation of Hebei Province (no. C2020206027 to FZ); 100 foreign experts of Hebei Province; Top talent100 foreign Experts program of Hebei Province; Biotechnology and Biological Sciences Research Council (no. BB/R003068/1 and BB/R02104X/1 to NG); Key Natural Science Foundation Projects of Hebei Province (no. H2019206028 to MH).

Declaration of interests

The authors declare that there are no conflicts of interest.

Author's contributions

XF, YW and ZC performed the experiments and data analyses. MH and FZ designed the experiments. MH, FZ and NG wrote the paper. All authors have read and approved the content of the manuscript.

Reference

[1] Quintana R A, Taylor W R, Cellular Mechanisms of Aortic Aneurysm Formation, Circ. Res. 124 (2019) 607-618.

[2] Hansson G K, Inflammation and Atherosclerosis: The End of a Controversy, Circulation. 136 (2017) 1875-1877.

[3] Marx S O, Totary-Jain H, Marks A R, Vascular smooth muscle cell proliferation in restenosis, Circ. Cardiovasc. Interv. 4 (2011) 104-11.

[4] Chaabane C, Otsuka F, Virmani R, Bochaton-Piallat M L, Biological responses in stented arteries, Cardiovasc. Res. 99 (2013) 353-63.

[5] Nordon I M, Hinchliffe R J, Loftus I M, Thompson M M, Pathophysiology and epidemiology of abdominal aortic aneurysms, Nat. Rev. Cardiol. 8 (2011) 92-102.

[6] Queisser N, Schupp N, Aldosterone, oxidative stress, and NF-κB activation in hypertension-related cardiovascular and renal diseases, Free Radic. Biol. Med. 53 (2012) 314-27.

[7] Chen H Z, Wang F, Gao P, Pei J F, Liu Y, Xu T T, Tang X, Fu W Y, Lu J, Yan Y F, Wang X M, Han L, Zhang Z Q, Zhang R, Zou M H, Liu D P, Age-Associated Sirtuin 1 Reduction in Vascular Smooth Muscle Links Vascular Senescence and Inflammation to Abdominal Aortic Aneurysm, Circ. Res. 119 (2016) 1076-1088.

[8] Chen G, Goeddel D V, TNF-R1 signaling: a beautiful pathway, Science. 296 (2002) 1634-5.

[9] Wajant H, Scheurich P, TNFR1-induced activation of the classical NF-κB pathway, FEBS J. 278 (2011) 862-76.

[10] Ting A T, Bertrand M J M, More to Life than NF-κB in TNFR1 Signaling, Trends Immunol. 37 (2016) 535-545.

[11] Wright A B, Sukhanova K Y, Elmslie K S, K(V)7 channels are potential regulators of the exercise pressor reflex, J. Neurophysiol. 126 (2021) 1-10.

[12] Barrese V, Stott J B, Greenwood I A, KCNQ-Encoded Potassium Channels as Therapeutic Targets, Annu. Rev. Pharmacol. Toxicol. 58 (2018) 625-648.

[13] Greenwood I A, Stott J B, The Gβ1 and Gβ3 Subunits Differentially Regulate Rat

Vascular Kv7 Channels, Front. Physiol. 10 (2019) 1573.

[14] Cheng J, Wen J, Wang N, Wang C, Xu Q, Yang Y, Ion Channels and Vascular Diseases, Arterioscler. Thromb. Vasc. Biol. 39 (2019) e146-e156.

[15] Jepps T A, Chadha P S, Davis A J, Harhun M I, Cockerill G W, Olesen S P, Hansen R S, Greenwood I A, Downregulation of Kv7.4 channel activity in primary and secondary hypertension, Circulation. 124 (2011) 602-11.

[16] Ohya S, Sergeant G P, Greenwood I A, Horowitz B, Molecular variants of KCNQ channels expressed in murine portal vein myocytes: a role in delayed rectifier current, Circ. Res. 92 (2003) 1016-23.

[17] Tsai Y M, Jones F, Mullen P, Porter K E, Steele D, Peers C, Gamper N, Vascular Kv7 channels control intracellular Ca^{2+} dynamics in smooth muscle, Cell Calcium. 92 (2020) 102283.

[18] Mani B K, Robakowski C, Brueggemann L I, Cribbs L L, Tripathi A, Majetschak M, Byron K L, Kv7.5 Potassium Channel Subunits Are the Primary Targets for PKA-Dependent Enhancement of Vascular Smooth Muscle Kv7 Currents, Mol. Pharmacol. 89 (2016) 323-34.

[19] Tykocki N R, Boerman E M, Jackson W F, Smooth Muscle Ion Channels and Regulation of Vascular Tone in Resistance Arteries and Arterioles, Compr Physiol. 7 (2017) 485-581.

[20] Li T, Wu K, Yue Z, Wang Y, Zhang F, Shen H, Structural Basis for the Modulation of Human KCNQ4 by Small-Molecule Drugs, Mol. Cell. 81 (2021) 25-37.

[21] Stott J B, Jepps T A, Greenwood I A, K(V)7 potassium channels: a new therapeutic target in smooth muscle disorders, Drug Discov. Today. 19 (2014) 413-24.

[22] Xia X, Zhang Q, Jia Y, Shu Y, Yang J, Yang H, Yan Z, Molecular basis and restoration of function deficiencies of Kv7.4 variants associated with inherited hearing loss, Hear. Res. 388 (2020) 107884.

[23] Gan S, Qiu S, Feng Y, Zhang Y, Qian Q, Wan Z, Tang J, Identification of genes associated with the effect of inflammation on the neurotransmission of vascular

smooth muscle cell, Exp. Ther. Med. 13 (2017) 1303-1312.

[24] Kharkovets T, Dedek K, Maier H, Schweizer M, Khimich D, Nouvian R, Vardanyan V, Leuwer R, Moser T, Jentsch T J, Mice with altered KCNQ4 K^+ channels implicate sensory outer hair cells in human progressive deafness, EMBO J. 25 (2006) 642-52.

[25] Kumar A, Lindner V, Remodeling with neointima formation in the mouse carotid artery after cessation of blood flow, Arterioscler. Thromb. Vasc. Biol. 17 (1997) 2238-44.

[26] Zhao G, Fu Y, Cai Z, Yu F, Gong Z, Dai R, Hu Y, Zeng L, Xu Q, Kong W, Unspliced XBP1 Confers VSMC Homeostasis and Prevents Aortic Aneurysm Formation via FoxO4 Interaction, Circ. Res. 121 (2017) 1331-1345.

[27] Yamanouchi D, Morgan S, Stair C, Seedial S, Lengfeld J, Kent K C, Liu B, Accelerated aneurysmal dilation associated with apoptosis and inflammation in a newly developed calcium phosphate rodent abdominal aortic aneurysm model, J. Vasc. Surg. 56 (2012) 455-61.

[28] Zhou H X, Xia X G, Xu Z S, An RNA polymerase II construct synthesizes short-hairpin RNA with a quantitative indicator and mediates highly efficient RNAi, Nucleic Acids Res. 33 (2005)

[29] Gu W D, Hong X C, Le Bras A, Nowak W N, Bhaloo S I, Deng J C, Xie Y, Hu Y H, Ruan X Z, Xu Q B, Smooth muscle cells differentiated from mesenchymal stem cells are regulated by microRNAs and suitable for vascular tissue grafts, J. Biol. Chem. 293 (2018) 8089-8102.

[30] Zhang Y X, Murugesan P, Huang K, Cai H, NADPH oxidases and oxidase crosstalk in cardiovascular diseases: novel therapeutic targets, Nature Reviews Cardiology. 17 (2020) 170-194.

[31] Zhou H, Xia X G, Xu Z, An RNA polymerase II construct synthesizes short-hairpin RNA with a quantitative indicator and mediates highly efficient RNAi, Nucleic Acids Res. 33 (2005) e62.

[32] Gu W, Hong X, Le Bras A, Nowak W N, Issa Bhaloo S, Deng J, Xie Y, Hu Y, Ruan X Z, Xu Q, Smooth muscle cells differentiated from mesenchymal stem

cells are regulated by microRNAs and suitable for vascular tissue grafts, J. Biol. Chem. 293 (2018) 8089-8102.

[33] Shambharkar P B, Blonska M, Pappu B P, Li H, You Y, Sakurai H, Darnay B G, Hara H, Penninger J, Lin X, Phosphorylation and ubiquitination of the IkappaB kinase complex by two distinct signaling pathways, EMBO J. 26 (2007) 1794-805.

[34] Schroeder B C, Hechenberger M, Weinreich F, Kubisch C, Jentsch T J, KCNQ5, a novel potassium channel broadly expressed in brain, mediates M-type currents, J. Biol. Chem. 275 (2000) 24089-95.

[35] Suna G, Wojakowski W, Lynch M, Barallobre-Barreiro J, Yin X, Mayr U, Baig F, Lu R, Fava M, Hayward R, Molenaar C, White S J, Roleder T, Milewski K P, Gasior P, Buszman P P, Buszman P, Jahangiri M, Shanahan C M, Hill J, Mayr M, Extracellular Matrix Proteomics Reveals Interplay of Aggrecan and Aggrecanases in Vascular Remodeling of Stented Coronary Arteries, Circulation. 137 (2018) 166-183.

[36] Schillinger M, Minar E, Restenosis after percutaneous angioplasty: the role of vascular inflammation, Vasc Health Risk Manag. 1 (2005) 73-8.

[37] Potente M, Gerhardt H, Carmeliet P, Basic and therapeutic aspects of angiogenesis, Cell. 146 (2011) 873-87.

[38] Aortic Wall Inflammation Predicts Abdominal Aortic Aneurysm Expansion, Rupture, and Need for Surgical Repair, Circulation. 136 (2017) 787-797.

[39] Dai Z, Zhu M M, Peng Y, Machireddy N, Evans C E, Machado R, Zhang X, Zhao Y Y, Therapeutic Targeting of Vascular Remodeling and Right Heart Failure in Pulmonary Arterial Hypertension with a HIF-2α Inhibitor, Am. J. Respir. Crit. Care Med. 198 (2018) 1423-1434.

[40] Brown I a M, Diederich L, Good M E, Delalio L J, Murphy S A, Cortese-Krott M M, Hall J L, Le T H, Isakson B E, Vascular Smooth Muscle Remodeling in Conductive and Resistance Arteries in Hypertension, Arterioscler. Thromb. Vasc. Biol. 38 (2018) 1969-1985.

[41] Chen P B, Black A S, Sobel A L, Zhao Y, Mukherjee P, Molparia B, Moore N E,

Aleman Muench G R, Wu J, Chen W, Pinto A F M, Maryanoff B E, Saghatelian A, Soroosh P, Torkamani A, Leman L J, Ghadiri M R, Directed remodeling of the mouse gut microbiome inhibits the development of atherosclerosis, Nat. Biotechnol. 38 (2020) 1288-1297.

[42] Falk E, Pathogenesis of atherosclerosis, J. Am. Coll. Cardiol. 47 (2006) C7-12.

[43] Forrester S J, Booz G W, Sigmund C D, Coffman T M, Kawai T, Rizzo V, Scalia R, Eguchi S, Angiotensin II Signal Transduction: An Update on Mechanisms of Physiology and Pathophysiology, Physiol. Rev. 98 (2018) 1627-1738.

[44] Sun J, Deng H, Zhou Z, Xiong X, Gao L, Endothelium as a Potential Target for Treatment of Abdominal Aortic Aneurysm, Oxid. Med. Cell. Longev. 2018 (2018) 6306542.

[45] Di Lorenzo A, Manes T D, Davalos A, Wright P L, Sessa W C, Endothelial reticulon-4B (Nogo-B) regulates ICAM-1-mediated leukocyte transmigration and acute inflammation, Blood. 117 (2011) 2284-95.

[46] Fontán-Lozano A, Suárez-Pereira I, Delgado-García J M, Carrión A M, The M-current inhibitor XE991 decreases the stimulation threshold for long-term synaptic plasticity in healthy mice and in models of cognitive disease, Hippocampus. 21 (2011) 22-32.

[47] Barrese V, Stott J B, Figueiredo H B, Aubdool A A, Hobbs A J, Jepps T A, Mcneish A J, Greenwood I A, Angiotensin II Promotes K(V)7.4 Channels Degradation Through Reduced Interaction With HSP90 (Heat Shock Protein 90), Hypertension. 71 (2018) 1091-1100.

[48] Linley J E, Rose K, Patil M, Robertson B, Akopian A N, Gamper N, Inhibition of M current in sensory neurons by exogenous proteases: a signaling pathway mediating inflammatory nociception, J. Neurosci. 28 (2008) 11240-9.

[49] Greene D L, Kosenko A, Hoshi N, Attenuating M-current suppression in vivo by a mutant Kcnq2 gene knock-in reduces seizure burden and prevents status epilepticus-induced neuronal death and epileptogenesis, Epilepsia. 59 (2018) 1908-1918.

[50] Sevilla-Montero J, Labrousse-Arias D, Fernández-Pérez C, Fernández-Blanco L,

Barreira B, Mondéjar-Parreño G, Alfaro-Arnedo E, López I P, Pérez-Rial S, Peces-Barba G, Pichel J G, Peinado V I, Cogolludo Á, Calzada M J, Cigarette Smoke Directly Promotes Pulmonary Arterial Remodeling and Kv7.4 Channel Dysfunction, Am. J. Respir. Crit. Care Med. 203 (2021) 1290-1305.